Journal of the European Ceramic Society 17 (1997) 1003–1010

PII: S0955-2219(96)00185-9
0955-2219/97/$17.00

Synergistic Strengthening and Toughening of Zircon Ceramics by the Additions of SiC Whisker and 3Y-TZP Simultaneously

Ying Shi, Xiaoxian Huang & Dongsheng Yan

Shanghai Institute of Ceramics, Chinese Academy of Sciences, 1295 Dingxi Road, 200050 Shanghai, People's Republic of China

(Received 9 May 1996; revised version received 28 August 1996; accepted 29 August 1996)

Abstract

The strengthening and toughening behaviours of SiC whiskers and tetragonal zirconia particles (3Y-TZP) in a zircon matrix were investigated. The results showed that the addition of SiC whiskers or 3Y-TZP could improve mechanical properties to some extent. The flexural strength and fracture toughness of 30 vol% SiC(w)/$ZrSiO_4$ reached 460 MPa and 4·7 MPa $m^{1/2}$, while the flexural strength and fracture toughness of 20 vol% 3Y-TZP/$ZrSiO_4$ were 410 MPa and 4·3 MPa $m^{1/2}$. Furthermore, when SiC whiskers and 3Y-TZP were introduced into the zircon matrix simultaneously, a drastic improvement in mechanical properties was achieved and a positive synergistic toughening effect was observed, showing that the combined toughening effect of SiC(w) and 3Y-TZP together was bigger than the sum of the individual toughening effects when either reinforcement acted alone. The flexural strength and fracture toughness of 30 vol% SiC(w)/20 vol% 3Y-TZP/$ZrSiO_4$ were 580 MPa and 7·0 MPa $m^{1/2}$ at room temperature, which were 90% and 130% higher than those of monolithic zircon and could be maintained up to 800°C. The microstructural observations by SEM and phase analysis by XRD demonstrated that the synergistic toughening effect was engendered from the interaction between microcrack toughening mechanism of 3Y-TZP and crack deflection, interfacial debonding as well as whisker pull-out by SiC whisker. © *1997 Elsevier Science Limited.*

1 Introduction

Ceramic matrix composites reinforced by different types of reinforcements have a potential to overcome some serious problems encountered in the applications of monolithic ceramic materials. Over the past one decade, various kinds of ceramic matrix composites have been extensively investigated regarding the enhancement of their mechanical properties, especially fracture toughness and flexural strength. Nowadays, more and more researchers have begun to utilize more than one kind of reinforcement to fabricate ceramic matrix composites in order to improve the mechanical properties of ceramics materials to a greater degree. For example, the incorporation of SiC whiskers combined with tetragonal zirconia particles (Y-TZP) in mullite matrix[1] and SiC whiskers combined with SiC particles in silicon nitride matrix[2] have been reported. Some results indicated that the combination of multiple reinforcements would achieve a better toughening and strengthening effect than the sum of the effects obtained by either reinforcement alone. Thus this method has become one of the leading trends to explore the toughening and strengthening of ceramic materials.

Recently, zircon ceramic ($ZrSiO_4$) has been recognized as a potential structural material for high-temperatures applications.[3,4] It has the merits of low thermal expansion coefficient ($4{\cdot}1 \times 10^{-6}\ °C^{-1}$ between 25°C and 1400°C), low thermal conductivity (4 $W\ m^{-1}\ °C^{-1}$ at room temperature), good chemical stability, excellent thermal shock resistance as well as good strength retention to high temperatures. However, its low flexural strength (200–300 MPa) and fracture toughness (2–3 MPa $m^{1/2}$) prevent its successful applications in practice. It has been reported that the mechanical properties of zircon can be improved by the addition of SiC whiskers[5] and SiC filament.[6] For example, in SiC(w)/$ZrSiO_4$ composite system, the flexural strength and fracture toughness could be increased from 300 MPa and 2 MPa $m^{1/2}$ for pure zircon

to 460 MPa and 4 MPa $m^{1/2}$ respectively under optimized processing conditions.[5]

In this paper, the fabrication of SiC(w)/$ZrSiO_4$ and 3Y-TZP/$ZrSiO_4$ composites is reported to investigate the strengthening and toughening effects of SiC whiskers and 3Y-TZP on zircon matrix, respectively. Furthermore, SiC whiskers and 3Y-TZP were added simultaneously into the zircon matrix to prepare (SiC(w)+3Y-TZP)/$ZrSiO_4$ composites for a better improvement of mechanical properties. The toughening behaviours of different reinforcing agents, especially the interaction between various toughening mechanisms arising from different reinforcements are discussed on the basis of the measurement of mechanical properties, microstructural observations and phase analysis.

2 Experimental Procedure

The zircon powder used was synthesized by a wet chemical method starting from $ZrOCl_2$ solution and fumed SiO_2. The details of the synthetic process have been described elsewhere.[7,8] Its chemical composition is shown in Table 1. Figure 1 displays its TEM morphology, showing that the average primary particle size was about 0·2–0·3 μm. The SiC whisker used was prepared in Shanghai Institute of Ceramics with a length in the range of 20–40 μm and a diameter in the range of 1–2 μm. The composition of the SiC whisker was as follows: Si:69·41 wt%, C: 29·13 wt%, CaO: 0·63 wt%, Al_2O_3: 0·40 wt%, Co_2O_3: 0·18 wt%, and Fe_2O_3: 0·084 wt%. 3Y-TZP powder was prepared by a co-precipitation method in the laboratory.

Table 1. Chemical composition of zircon powder

Composition	ZrO_2	SiO_2	HfO_2	Al_2O_3	MgO	Fe_2O_3
Content (wt%)	67·22	30·85	1·39	0·11	0·014	0·029

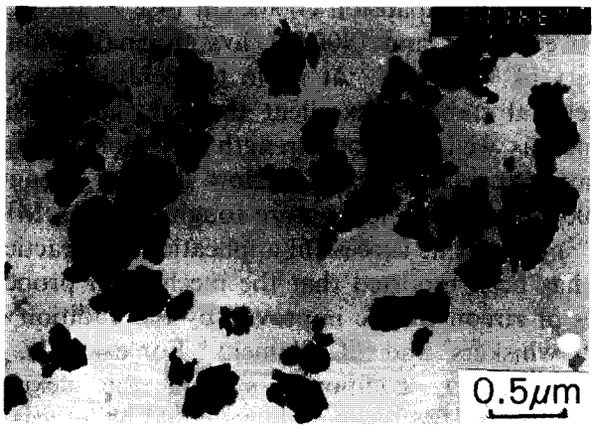

Fig. 1. TEM micrograph of zircon powder.

The primary particle size of 3Y-TZP powder was about 20–30 nm, and the specific surface area was about 30 $m^2 g^{-1}$.

The zircon powder, SiC whisker and 3Y-TZP powder were mixed in the desired volume ratio by wet milling for 24 h using distilled water as dispersion solvent in a polyethylene container. The milling media were 3Y-TZP balls with a diameter of 5–6 mm. After drying in an oven, the mixed powder was sieved to pass 40 mesh, and hot-pressed in a BN-coated graphite die for densification, which was carried out at 1600°C for 1 h in a nitrogen atmosphere under a pressure of 30 MPa.

The hot-pressed zircon matrix composites were cut and ground into 2·5 × 5 × 30 mm^3 rectangular bars with a diamond wheel. The flexural strength was measured by a three-point bending test at a crosshead speed of 0·5 mm min^{-1} with a span of 20 mm. Test specimens of dimensions 5 × 2·5 × 30 mm^3 were prepared for fracture toughness measurement by single edge notched beam (SENB) method. The notches used were 0·2–0·25 mm wide and 2·5 mm in depth. The SENB specimens were fractured by three-point bending at a crosshead speed of 0·05 mm min^{-1} with a span of 20 mm.

Scanning electron microscopy (SEM) and transmission electron microscopy (TEM) were adopted to observe the crack propagation path, fracture surfaces and microstructural features of the composites. The morphology of the grain boundary phase in the composite was observed by high resolution electron microscopy (HREM). The phase composition in zircon matrix composites was detected by X-ray diffraction (XRD) method. The ratio of tetragonal zirconia ($f*$) was determined by the following equation:

$$f* = I_{t(111)}/[I_{m(11\bar{1})} + I_{m(111)} + I_{t(111)}]$$

where I is the peak intensity of XRD, m and t stand for monolithic and tetragonal phase, respectively.

3 Results and Discussion

3.1 SiC(w)/$ZrSiO_4$ composite

3.1.1 Mechanical properties

Figure 2 illustrates the effect of SiC whisker content on the relative density of the SiC(w)/$ZrSiO_4$ composites. The relative density decreases gradually with increasing SiC whisker addition. For 30 vol% SiC(w)/$ZrSiO_4$ composite, the relative density still has a value of 96·2%, but it drops drastically to 82% when the content of SiC whisker reaches 40 vol%. This phenomenon is due to the common existence of SiC whisker segregation in

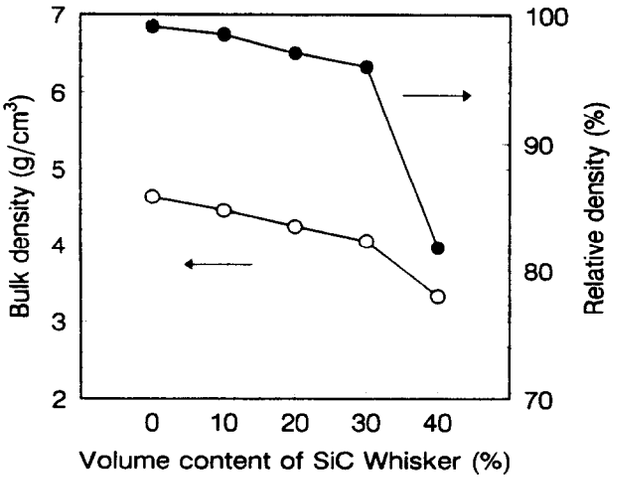

Fig. 2. The dependence of relative density of SiC(w)/$ZrSiO_4$ on the content of SiC(w).

the composite, which was attributed to the difficulty in dispersing SiC whisker homogeneously at high SiC whisker content. The SEM morphologies of fracture surfaces for SiC(w)/$ZrSiO_4$ composites with 20 vol% and 40 vol% SiC whisker content are displayed in Fig. 3, showing intergranular fracture mode for both specimens whereas the densification levels for different compositions were quite different. Figure 3(A) shows that SiC(w)/$ZrSiO_4$ composites with 20 vol% whisker have already been fully densified with a uniform microstructure, whereas there obviously exist clusters of SiC whisker on the fracture surface of 40 vol% SiC(w)/$ZrSiO_4$, accompanied by a relatively large amount of pores with size of about 5–10 μm. The differences between the microstructure features on fracture surfaces agrees with the dependence of relative density of SiC(w)/$ZrSiO_4$ composites on SiC(w) content.

Figure 4 shows the effects of SiC(w) content on the flexural strength and fracture toughness of SiC(w)/$ZrSiO_4$. The flexural strength and fracture toughness of SiC(w)$ZrSiO_4$ increase monotonously as SiC(w) content increases from 0 to 30 vol%. For 30 vol% SiC(w)/$ZrSiO_4$, the average flexural strength and fracture toughness reach 480 MPa and 4·7 MPa $m^{1/2}$, which are both 60% higher than those of monolithic zircon ceramics. When the SiC(w) content exceeds 30 vol%, the changing laws of flexural strength and fracture toughness are different. The flexural strength drops to 420 MPa due to the sensitivity of flexural strength to the decrease of relative density. However, the fracture toughness of composites increases to 5·3 MPa $m^{1/2}$ continuously because the fracture toughness is not so sensitive to the reduction of relative density as flexural strength is; on the contrary, the existence of pores would lower the stress concentration at the tip of the crack. As a result,

Fig. 3. SEM micrographs of fracture surface of (A) 20 vol% SiC(w)/$ZrSiO_4$ and (B) 40 vol% SiC(w)/$ZrSiO_4$.

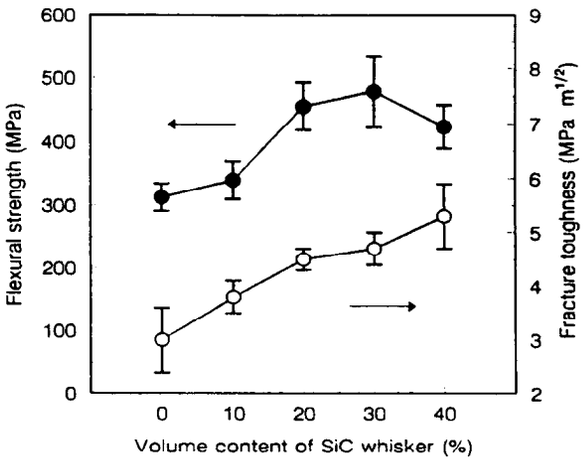

Fig. 4. The dependence of flexural strength and fracture toughness of SiC(w)/$ZrSiO_4$ composite on the content of SiC(w).

the fracture toughness increases further when the content of SiC(w) reaches 40 vol%.

3.1.2 TEM observations and toughening mechanisms of SiC(w)/$ZrSiO_4$ composite

From the different types of toughening behaviour of SiC whisker in zircon matrix shown in Fig. 5, we can discuss the toughening mechanisms existing in SiC(w)/$ZrSiO_4$ composites. Normally, the whiskers in the composites have axes either normal or inclined to the crack plane. In Fig. 5(A), the tip of crack was pinned by the SiC whisker because the propagating direction of the crack was vertical to the SiC whisker which was able to take advantage of high strength and modulus of the SiC whisker. When the propagating direction of the crack was almost parallel to the whisker, the crack tended to deflect by the SiC whisker at the interface between SiC(w) and zircon, accompanied by the interfacial debonding which is shown in Figs 5(B) and (C). Moreover, the typical SEM micrographs shown in Fig. 3(A) indicated that whisker pull-out was also an operating toughening mechanism. In terms of a slight mismatch of the thermal expansion coefficient of zircon ($4{\cdot}1 \times 10^{-6}$ °C^{-1}) and SiC whisker ($4{\cdot}7 \times 10^{-6}$ °C^{-1}), a weak tensile stress would exist at the interfaces between the SiC whisker and zircon grain after the hot-pressing process, which is favourable to the occurrence of interfacial debonding and whisker pull-out during fracture. So it could be concluded that crack deflection, interfacial debonding, whisker pull-out and crack pinning were the main toughening mechanisms in SiC(w)/$ZrSiO_4$ composites.

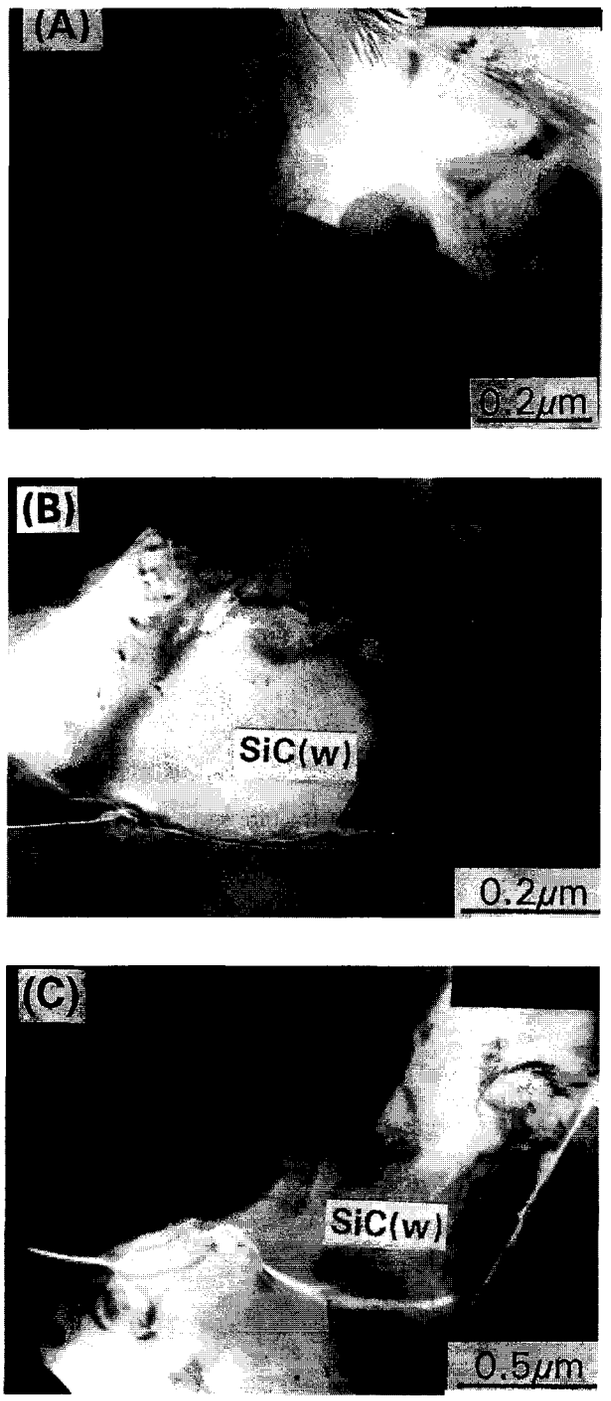

Fig. 5. TEM micrographs of SiC(w)/$ZrSiO_4$ showing (A) crack pinning, (B) and (C) crack deflection and interfacial debonding.

3.2 3Y-TZP/$ZrSiO_4$ composite

Table 2 gives a comparison of relative density and mechanical properties between monolithic zircon and 20 vol% 3Y-TZP/$ZrSiO_4$ composite. It can be seen from the data of relative density that the addition of 3Y-TZP does not hinder the densification of zircon. The average flexural strength and fracture toughness of 20 vol% 3Y-TZP/$ZrSiO_4$ were 410 MPa and 4·3 MPa $m^{1/2}$, which were 30–40% higher than those of monolithic zircon.

Figure 6(A) shows that the zircon grain in 20 vol% 3Y-TZP/$ZrSiO_4$ appeared to be equiaxed in shape with a size of about 0·5 μm, which was finer than that of monolithic zircon. Usually, the size of zircon grain in monolithic zircon ceramics is about 1 μm. This effect could be attributed to the existence of intergranular 3Y-TZP grains, which act as grain growth inhibitors, suppressing the grain growth of zircon in the hot-pressing process. Furthermore, some microcracks were observed at the interfaces between zircon grain and ZrO_2 grain with twin structure (Fig. 6(B)), proving the occurrence of T-ZrO_2 → m-ZrO_2 phase transformation.

Table 2. Comparison of relative density and mechanical properties between monolithic zircon and 20 vol% 3Y-TZP/$ZrSiO_4$

	Monolithic zircon	*20 vol% 3Y-TZP/$ZrSiO_4$*
Relative density (%)	99·1	99·2
Flexural strength (MPa)	310	410
Fracture toughness (MPa $m^{1/2}$)	3·0	4·3

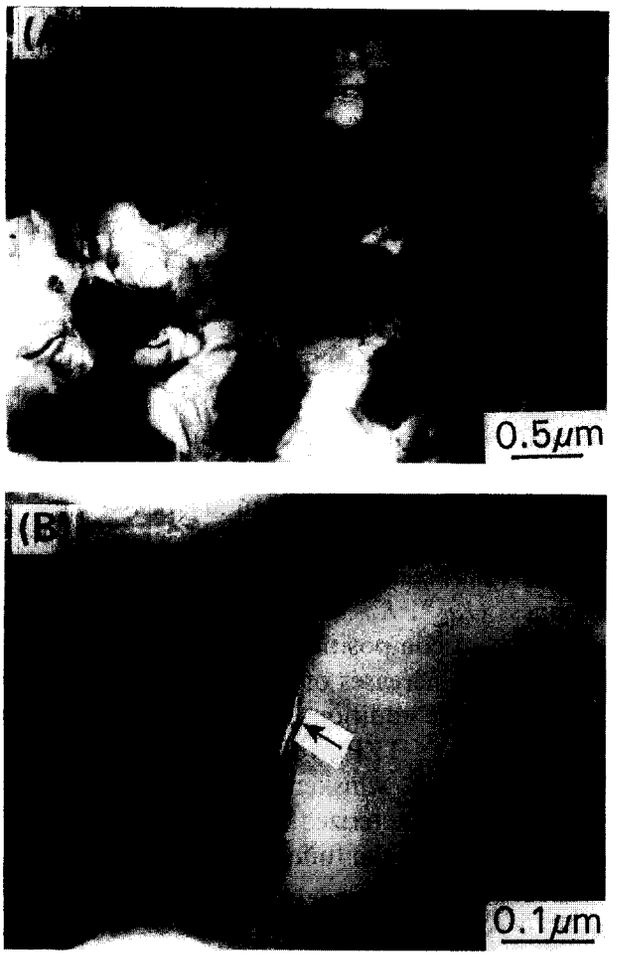

Fig. 6. (A) TEM micrograph of 20 vol% 3Y-TZP/$ZrSiO_4$ composite. (B) Microcrack in 20 vol% 3Y-TZP/$ZrSiO_4$ composite.

In order to determine the percentage of transformable tetragonal ZrO_2 during fracture (f_t) in 20 vol% 3Y-TZP/$ZrSiO_4$, an XRD method was used to measure the percentage of T-ZrO_2 on the polished surface of the composite specimen (f_s) and in the ground powder of sintered composite (f_p), which stand for the percentage of T-ZrO_2 in 20 vol% 3Y-TZP/$ZrSiO_4$ before and after fracture, respectively. The data listed in Table 3 show that 24·9% of T-ZrO_2 has transformed during fracture. As a result, microcracks will generate around the tranformed ZrO_2 grains, which is shown in Fig. 6(B).

The results of TEM and XRD suggested that microcrack toughening and phase transformation toughening were two active toughening mechanisms in 20 vol% 3Y-T7P/$ZrSiO_4$. The microcracks would interact with the main crack to shield the main crack tip and lower the stress concentration at the crack tip, resulting in the improvement of mechanical properties. As for the phase transformation mechanism, it may be argued that it was not the dominant toughening mechanism because the Young's modulus and strength of zircon matrix were quite low.[10] The high-temperature mechanical properties discussed below will support this point strongly.

Table 3. Percentage of transormable T-ZrO_2 in 20 vol% 3Y-TZP/$ZrSiO_4$ during fracture

Percentage of T-ZrO_2 on polished surface of composite (f_s)	*Percentage of T-ZrO_2 in ground powder of composite* (f_p)	*Percentage of tranformable T-ZrO_2 during fracture* ($f_t=f_s-f_p$)
66·5%	41·6%	24·9%

3.3 SiC(w)/3Y-TZP/$ZrSiO_4$ composite

3.3.1 Mechanical properties

Zircon matrix composites with the incorporation of both SiC(w) and 3Y-TZP as two reinforcing agents were further investigated. The compositions of the composites were designed to be *x*vol%SiC(w) + 20 vol% 3Y-TZP+(100-20-*x*) vol% $ZrSiO_4$. The effects of the content of added SiC(w) on the mechanical properties of composites are illustrated in Fig. 7. The flexural strength and fracture toughness of composites are found to increase with increasing contents of SiC(w), showing a high flexural strength of 580 MPa and a high fracture toughness of 7·0 MPa $m^{1/2}$ at 30 vol% SiC whisker addition.

The temperature dependence of flexural strength was investigated for the composition of 30 vol% SiC(w)/20 vol% 3Y-TZP/$ZrSiO_4$ and the results are shown in Fig. 8. The data for monolithic zircon are also plotted for a comparison. The flexural strength of composites is almost constant from room temperature to 800°C. It begins to decrease gradually in the temperature range of 800°C–1000°C, followed by a drastic degradation when temperature is above 1000°C. The value of

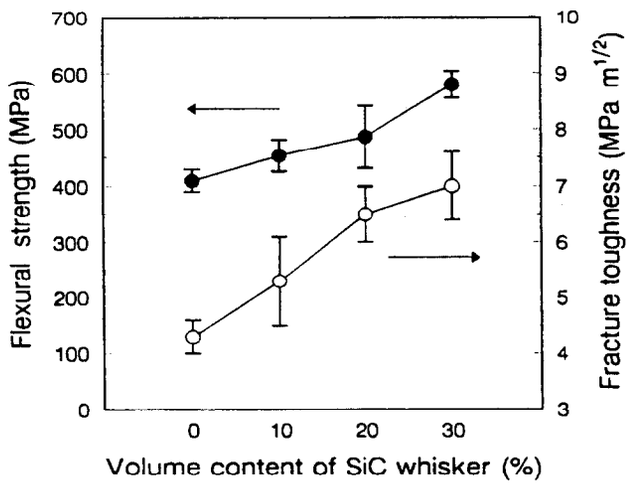

Fig. 7. The dependence of flexural strength and fracture toughness of SiC(w)/3Y-TZP/$ZrSiO_4$ on the content of SiC whisker.

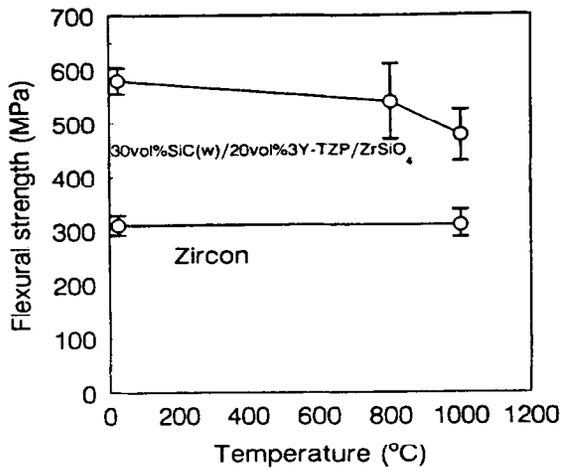

Fig. 8. The dependence of flexural strength of 30 vol% SiC(w)/20 vol% 3Y-TZP/$ZrSiO_4$ on temperature.

flexural strength of the composite is 480 MPa at 1000°C, which is 60% higher than that of pure zircon. The HREM micrograph displayed in Fig. 9 shows that a layer of glassy phase with a thickness of 1–2 nm exists at the interface between zircon grain and SiC whisker in the composite. It probably originates from the SiO_2 layer on the SiC whisker and other oxide impurities in the starting powder, which is responsible for the strength decrease of the composite at temperatures above 1000°C.

3.3.2 Synergistic toughening behaviour of SiC(w) and 3Y-TZP

In order to discuss the toughening mechanism in SiC(w)/3Y-TZP/$ZrSiO_4$ composite, the percentage of transformable tetragonal ZrO_2 in 30 vol% SiC(w)/20 vol% 3Y-TZP/$ZrSiO_4$ was determined by the same method as we have used for 20 vol% 3Y-TZP/$ZrSiO_4$ composite. The results listed in Table 4 indicated that the f_s and f_p in the 30 vol% SiC composite system are less than those in the previous one, showing that phase transformation toughening has weakened and microcrack toughening has enhanced in 30 vol% SiC(w)/20 vol% 3Y-TZP/$ZrSiO_4$. The results shown in Fig. 8 demonstrate that flexural strength of SiC(w)/3Y-TZP/$ZrSiO_4$ does not decrease obviously up to 800°C, which testifies that the phase transformation toughening is not the main toughening mechanism because it becomes invalid when temperature reaches 800°C due to the disappearance of driving force of T-ZrO_2 → m-ZrO_2.[11] So it can be concluded that microcrack toughening was the main toughening mechanism engendered by 3Y-TZP when SiC(w) and 3Y-TZP were introduced into zircon matrix simultaneously.

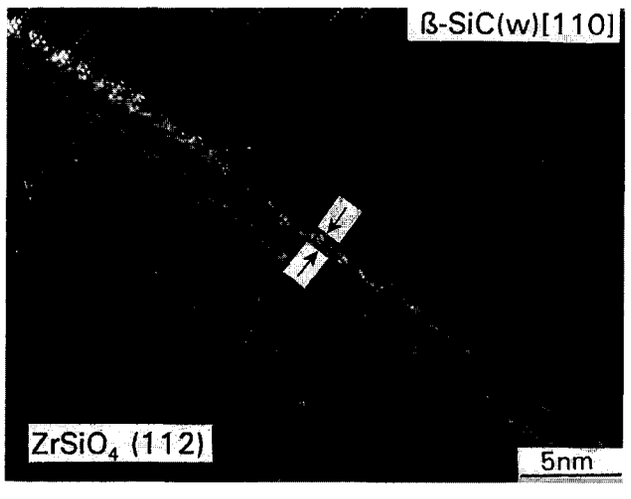

Fig. 9. The HREM micrograph of 30 vol% SiC(w)/20 vol% 3Y-TZP/$ZrSiO_4$ showing glassy phase existed at the interface between zircon grain and SiC(w).

To evaluate the toughening effect arising from different reinforcements, the increments of fracture toughness (K_{IC}^W, K_{IC}^Z and K_{IC}^{Z+W}) for composites with different compositions were calculated, which stand for the increases of fracture toughness originating from the additions of SiC whisker, 3Y-TZP and (SiC(w)+3Y-TZP), respectively. The synergistic effects of SiC whisker and 3Y-TZP in zircon matrix were characterized by the value K_{IC}^S, which was calculated by the following equation:

$$K_{IC}^S = K_{IC}^{Z+W} - K_{IC}^Z - K_{IC}^W$$

Table 5 lists the relevant results based on the mechanical properties plotted in Fig. 4, Fig. 7 and Table 2. It can be seen that the increases of K_{IC} when SiC(w) and 3Y-TZP are introduced into zircon together are larger than the sum of those when the SiC(w) and 3Y-TZP are introduced into zircon separately. The data of K_{IC}^S indicate that there exists a positive synergistic toughening effect when SiC(w) and 3Y-TZP are incorporated into zircon matrix simultaneously, and this synergistic effect is enhanced gradually as the content of SiC whisker is increased.

The synergistic toughening behaviour is closely related to the concurrent actions between the SiC whisker toughening and microcrack toughening by 3Y-TZP. Figures 10 and 11 display the SEM micrographs of fracture surfaces and crack propagation path on the polished surfaces for 30 vol% SiC(w)/$ZrSiO_4$ and 30 vol% SiC(w)/20 vol% 3Y-TZP/$ZrSiO_4$. Comparing the morphologies of fracture surfaces shown in Figs 10(A) and (B), it

Table 4. Percentage of transformable T-ZrO_2 in 30 vol% Sic(w)/20 vol% 3Y-TZP/$SrSiO_4$ during fracture

Percentage of T-ZrO_2 on polished surface of composite (f_s)	*Percentage of T-ZrO_2 in ground powder of composite* (f_p)	*Percentage of tranformable T-ZrO_2 during fracture* ($f_t=f_s-f_p$)
51·5%	34·9%	16·6%

Table 5. Increments of fracture toughness of zircon matrix composites arising from different contents of reinforcements (MPa $m^{1/2}$)

Composite	K_{IC}^{W}	K_{IC}^{Z}	K_{IC}^{Z+W}	K_{IC}^{S}
10 vol% SiC(w)	0·8		2·3	0·2
20 vol% SiC(w)	1·5		3·5	0·7
30 vol% SiC(w)	1·7		4·0	1·0
20 vol% 3Y-TZP		1·3		

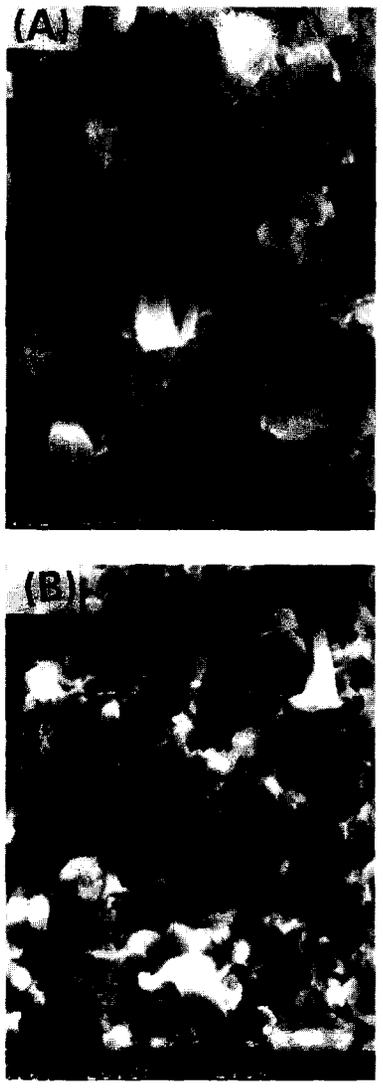

Fig. 10. SEM micrographs of fracture surface of (A) 30 vol% SiC(w)/$ZrSiO_4$ and (B) 30 vol% SiC(w)/20 vol% 3Y-TZP/$ZrSiO_4$.

was found that the fracture surface of the composite with SiC(w) and 3Y-TZP is rougher, with pull-out whiskers and the corresponding holes left, than that of composite with SiC(w) only. The crack-propagating path of 30 vol% SiC(w)/20 vol% 3Y-TZP/$ZrSiO_4$ (Fig. 11(B)) is much more tortuous than that of 30 vol% SiC(w)/$ZrSiO_4$ (Fig. 11(A)), suggesting that the crack path has been more strongly deflected by SiC(w) and 3Y-TZP simultaneously. Thus it could be deduced that the crack pinning, crack deflection, interfacial debonding and whisker pull-out arising from

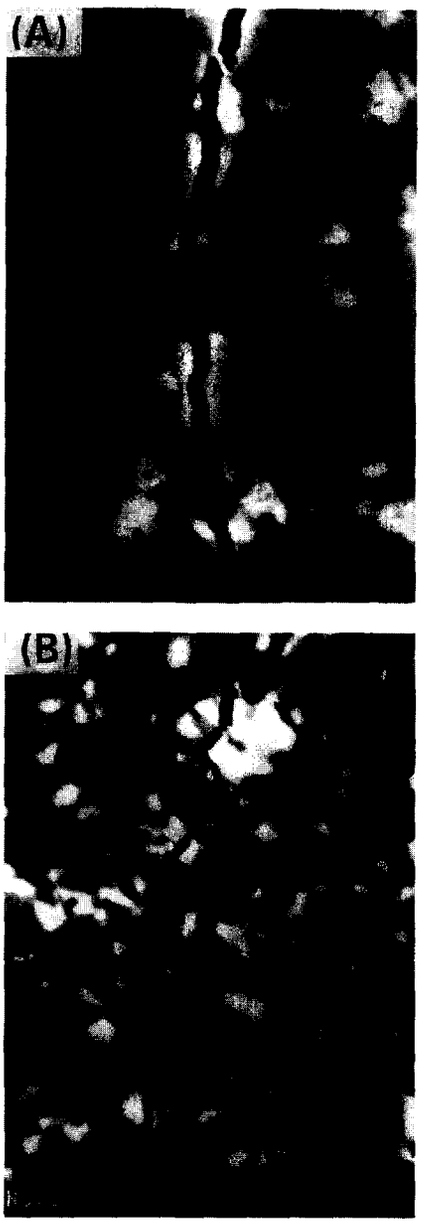

Fig. 11. SEM micrographs of crack propagation on the polished surfaces of (A) 30 vol% SiC(w)/$ZrSiO_4$ and (B) 30 vol% SiC(w)/20 vol% 3Y-TZP/$ZrSiO_4$.

SiC(w) and microcrack toughening can interact with each other when they act in the zircon matrix at the same time, resulting in the clear positive synergistic toughening effect.

4 Conclusion

This paper shows that zircon ceramics can be strengthened and toughened by the addition of SiC whisker and 3Y-TZP when properly processed. The incorporation of SiC whisker and 3Y-TZP into the zircon matrix together enhanced the mechanical properties of zircon dramatically, with a flexural strength of 580 MPa and a fracture toughness of 7·0 MPa $m^{1/2}$, respectively, which were about 90% and 130% higher than those of

monolithic zircon and could be maintained up to 800–1000°C. Moreover, it was found that the toughening effect arising from the simultaneous addition of SiC whisker and 3Y-TZP was larger than the sum of toughening effects arising from the SiC whisker and 3Y-TZP, respectively, indicating that there was a synergistic toughening effect in zircon matrix when SiC whisker and 3Y-TZP were introduced at the same time. On the basis of microstructural observations by SEM, TEM and XRD analysis, it is argued that this synergistic effect originated from the interaction between the toughening mechanisms of SiC whisker, such as crack deflection, interfacial debonding and whisker pull-out and microcrack mechanism by 3Y-TZP addition.

References

1. Robert, R., Mazdiyasni, K. S. & Mendiratta, M. G., *J. Am. Ceram. Soc.*, **71** (1988) 503.
2. Hironori, K., Takaaki, S., Hiroshi, S. *et al.*, *J. Am. Ceram. Soc.*, **73** (1990) 678.
3. Singh, R. N., *Am. Ceram. Soc. Bull.*, **70**[1] (1991) 55.
4. Mori, T., Yamamura, H., Kobayashi, H. *et al.*, *J. Am. Ceram. Soc.*, **75** (1992) 2420.
5. Kondih, I., Tanaka, T. & Tamari, N., *J. Ceram. Soc. Jpn*, **101**(3) (1993) 369.
6. Singh, R. N., *J. Am. Ceram. Soc.*, **73** (1990) 2399.
7. Shi, Y., Huang, X. X. & Yan, D. S., *Proc. 5th Inter. Sym. on Ceram. Mater. and Components for Engines*, 29 May–1 June 1994, Shanghai, China, p. 610.
8. Shi, Y., Huang, X. X. & Yan, D. S., *Mater. Lett.*, **21** (1994) 79.
9. Claussen, N., *J. Am. Ceram. Soc.*, **61** (1978) 85.
10. Lange, F. F., *J. Mater. Sci.*, **17** (1981) 225.
11. Claussen, N., *Mater. Sci. Engng*, **71** (1985) 23.